Nanomaterials for Solar Energy Conversion: Dye-Sensitized Solar Cells Based on Ruthenium (II) *Tris*-Heteroleptic Compounds or Natural Dyes

Juliana dos Santos de Souza, Leilane Oliveira Martins de Andrade and André Sarto Polo

Abstract The worldwide energy demand is growing and the development of sustainable power generation is a critical issue. Among several possibilities, dye-sensitized solar cells, DSSCs, have emerged as a promising device to meet the energy needs as an environmentally friendly alternative and investigation for academic and technological improvement of DSSCs are being carried out. One of the most important components of this device is the dye-sensitizer, since it is responsible for the sunlight harvesting and electron injection, the first steps of energy conversion. Herein, we review the developments on *tris*-heteroleptic ruthenium dye-sensitizers, which have been gaining much attention on the last years due to the possibility of modulating their photochemical and photophysical properties of the complex by using different ligands. Besides synthetic compounds, natural dyes have also been employed as semiconductor sensitizers for these devices and are also reviewed. These dyes can lower the device production costs since they can be promptly obtained from fruits or flowers in a very simple way. Among numerous classes of natural dyes, anthocyanins have been the most investigated ones and gained special attention in this work.

1 Aims and Scope

Dye-sensitized solar cells, DSSCs, gained much attention since it is a simple and cheap device capable of converting the sunlight into electricity through a regenerative photoelectrochemical process. DSSCs overall efficiency attained 11 % and it is estimated to last around 20 years. Besides the economic advantages, these

J. d. S. de Souza (✉) · L. O. M. de Andrade · A. S. Polo
Centro de Ciências Naturais e Humanas, Universidade Federal do ABC, Rua Santa Adélia 166, Santo André, SP 09210-170, Brazil
e-mail: andre.polo@ufabc.edu.br

F. L. de Souza and E. R. Leite (eds.), *Nanoenergy*,
DOI: 10.1007/978-3-642-31736-1_2,

devices can be transparent and allows their use for distinct architectonic purposes, such as facades of buildings. DSSCs are based on a nanocrystalline mesoporous semiconductor films sensitized by dyes, which are responsible for light harvesting and electron transfer, these processes, start the energy conversion and are directly responsible for its overall efficiency.

This chapter aims to review a specific class of synthetic dye, the *tris*-heteroleptic ruthenium sensitizers, which have been attracting much attention on the last years due to the possibility of tune their spectroscopic and electrochemical properties as well as to improve the stability of the device. The recent advances on the use of natural dyes as semiconductor sensitizers, from 2003 to 2010, are also reviewed.

2 Introduction

The use of fossil fuel based technologies is the major responsible for the continuous increase in the pollution and in the concentration of greenhouse gases. Renewable sources must have higher contribution on the energetic matrix in providing more energy available for the humanity in a short period, having low environmental impact [1, 2]. The interest on the conversion of environmentally friendly energy sources led to the development of several devices that took the advantage of the continuous evolution on several fields of research, which can result in new materials for already developed devices. For instance, the performance of direct methanol fuel cells, a well known technology [3, 4] was improved due to the development of nanomaterials especially designed for the energy conversion process [5, 6] and their evolution allows the use of light to boost the process through a synergic arrangement [7–10].

The use of sunlight has been gaining much attention due to its abundance. For instance, it is possible to supply human energy needs up to 2050 covering only 0.16 % of the earth surface with 10 % efficiency solar devices [1, 11]. There are several investigations on the conversion of sunlight in substances with more chemical energy than the reactants in a process that mimics the photosynthesis; this approach is known as artificial photosynthesis [12]. Most recently, the investigation on this research field is being called solar fuels and several papers were published describing photochemical approaches to produce high energy content substances, or fuels, from simple reactants such as water or CO_2 [13–19].

Great interest is dedicated to an especially attractive, the Dye-sensitized solar cells, DSSC, since they are capable of converting the sunlight into electricity based on photoelectrochemical principles. The materials employed for the construction of these new solar cells are common and cheap and the procedures do not require controlled environment, thus clean rooms or any other sophisticated control can be avoided, consequently a very low production cost is estimated (less than 1 € per Wp) [20]. The use of new nanomaterials allows interesting features of these devices, such as transparency, possibility to have distinct colors, among others. These characteristics are very interesting for new applications of solar cells, since

it can substitute glass windows and promote the co-generation of energy, or for any other architecture design.

Albeit the possible use of sensitization effect for solar energy conversion is known for a long time [21], the breakthrough of these solar cells was in 1991 when B. O'Reagan and M. Grätzel published the use of nanocrystalline and mesoporous TiO_2 film [22]. This film enhanced the light absorption due to its sponge-like characteristic which increases the surface area. The nanocrystallinity plays an important role on the electron injection and transport in these devices [23].

Since the paper of 1991, this field has been growing very fast and all the aspects of these solar cells are investigated [24–27]. In this review, the focus is on the development of *tris*-heteroleptic ruthenium (II) dyes as well as the use of natural extracts as a source of sensitizers. The absorption spectra and photoelectrochemical parameters published for these compounds since 2003 will be reviewed and discussed.

2.1 Dye-Sensitized Solar Cells: Principles and Operation

Dye-sensitized solar cells are prepared in a sandwich arrangement and are comprised by two electrodes, the photoanode and the counter-electrode, Fig. 1. The photoanode is a conducting glass covered by a mesoporous and nanocrystalline TiO_2 film, sensitized by the dye-sensitizers. The counter electrode is a conducting glass covered by a thin film of catalyst, such as platinum or graphite. Between these electrodes is placed a mediator layer, usually a solution of I_3^-/I^- in nitriles.

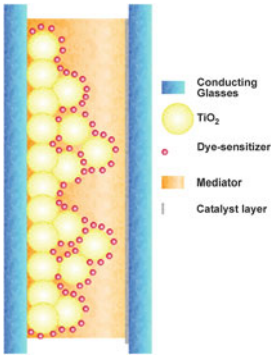

Fig. 1 Schematic arrangement of a dye-sensitized solar cell

In order to promote the energy conversion, the sunlight is harvested by the dye-sensitizers leading to an excited-state capable of inject an electron into the semiconductor conducting band. The oxidized dye is immediately regenerated by the mediator and the injected electron percolates through the semiconductor film, reaches the conducting glass and flows by the external circuit to the counter-electrode. The counter electrode is responsible for regenerating the oxidized specie of the mediator, reducing it by a catalyzed reaction using electrons from the

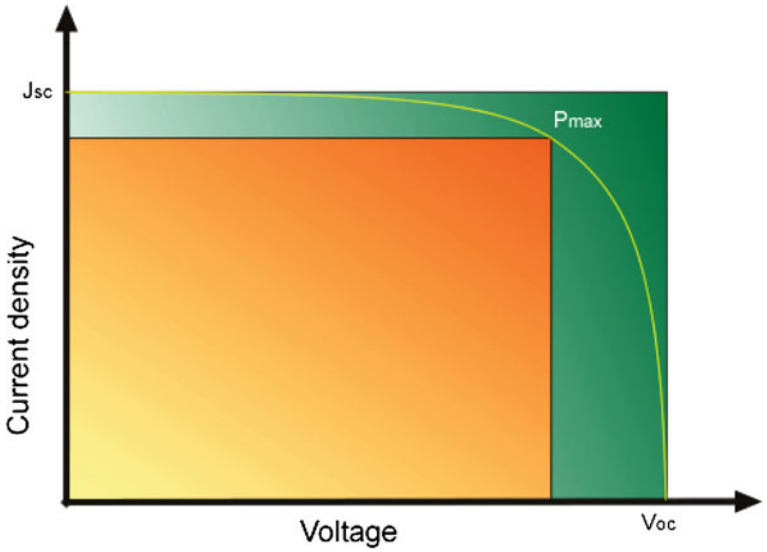

Fig. 2 Schematic current–voltage curve

external circuit. Since there is not a permanent chemical change for dye-sensitized solar cells, the estimated lifetime of these devices is 20 years [23].

2.2 Performance Experiments

Dye-sensitized solar cells are evaluated by several experimental approaches. For instance, the recombination processes or electron injection dynamics are investigated by time-resolved experiments [27–35], information about electron transport and electrical characteristics of TiO_2 film can be obtained by electrochemical impedance spectroscopy [36]. Among several experiments used in evaluation of DSSCs, two experiments play an important role for investigation of dye performance, the current–voltage curves and photocurrent action spectra. Due to their importance, they are detailed in the next sections.

2.2.1 Current–voltage (IxV) Curves

Current–voltage curves allow the access to one of the most important information about the prepared solar cells, the overall efficiency, η. Other important parameters such as the short circuit current density, J_{sc}, open-circuit potential, V_{oc}, and fill factor, ff, are also determined by this experiment. In most cases, IxV curves determined experimentally for dye-sensitized solar cells are similar to the schematic one, Fig. 2.

Short-circuit current density, J_{SC}, and open-circuit potential, V_{OC}, are the values determined by the intersection of IxV curve to the current density axis. The voltage at this axis is zero, the short-circuit condition, thus the current is named for this condition. Analogous idea is applied for the determination of open-circuit potential, since the current at voltage axis is zero, open circuit condition.

The maximum power output of a DSSC, P_{max}, is the highest value obtained for the multiplication of current density and voltage for each point of the IxV curve and can be graphically expressed as the area covered by the orange rectangle in of Fig. 2. On the other hand, the multiplication of V_{OC} by J_{SC} results in the maximum power output possible to be achieved for this DSSC and it can also be represented by the green rectangle of Fig. 2. The fill-factor, ff, is named for the amount of the green rectangle which is filled by the orange one and. Thus ff express the electrical losses of DSSCs. Mathematically, ff can be determined by the ratio of P_{max} and the multiplication of J_{SC} by V_{OC}, Eq. 1.

$$ff = \frac{P_{max}(mW \cdot cm^{-2})}{J_{sc}(mA.cm^{-2}) \cdot Voc(V)} \tag{1}$$

Under simulated solar irradiation condition (1 sun = P_{irr} = 100 mW cm^{-2}), the overall efficiency, η_{Cell}, can be determined by dividing P_{max} by the total incident light power, P_{irr}, Eq. 2, resulting in the percentage amount of solar light converted in electrical Output.

$$\eta\% = \frac{P_{max}}{P_{irr}} \cdot 100\ \% \tag{2}$$

2.2.2 Photocurrent Action Spectra

Photocurrent action spectra exhibit the photoelectrochemical behavior of solar cells as a function of wavelength. For each wavelength can be determined the incident photon-to-current conversion efficiency, IPCE, and the spectra are valuable to analyze the performance of new dyes prepared. IPCE values can be determined by a relationship that considers the energy and intensity of the incident light, the J_{SC} and Planck's constant, Eq. 3.

$$IPCE(\lambda) = \frac{J_{sc}}{P_{irr} \cdot e} \cdot \frac{hc}{\lambda} \tag{3}$$

J_{sc} Short-circuit photocurrent density (A m^{-2});
h Planck's constant (J s);
c Speed of light (m s^{-1});
λ Irradiation wavelength (nm);
P_{irr} Power of the incident light (W m^{-2});
e Elementary charge (C).
For practical purposes, this equation can be simplified to Eq. 4.

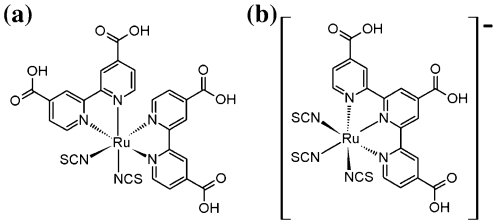

Fig. 3 Structures of the N3 (**a**) and black-dye (**b**) sensitizers

$$IPCE\ \%\ (\lambda) = \left(1239.8 \cdot \frac{J_{sc}(mA \cdot cm^{-2})}{P_{irr}(mW \cdot cm^{-2})\lambda(nm)}\right) \cdot 100\ \% \tag{4}$$

IPCE values are also related to some important parameters for DSSCs, such as light harvesting efficiency, LHE, electron injection quantum efficiency, Φ_{EI}, and the efficiency of collecting electrons in the external circuit, η_{EC}, Eq. 5 [37]. The simple measurements, such as J_{SC} and P_{irr} allow the access to important information such as the electron injection quantum yield.

$$IPCE(\lambda) = LHE\Phi_{E1}\eta_{EC} \tag{5}$$

Photocurrent action spectra are valuable experiments to evaluate new dye-sensitizers since it is possible to directly associate the absorption response of the dye with the conversion efficiency. This is valuable information for design new sensitizers.

2.3 Molecular Engineering

The design of new dye-sensitizers is based on joining in just one specie components capable of performing specific tasks. Using different ligands it is possible to have excellent light harvesting, electron injection on semiconductor conducting band and fast regeneration by the mediator. A new molecule to be employed in DSSCs should fulfill some basic requirements such as having an intense absorption on the visible region, which corresponds to 44 % of the incident sunlight on the earth's surface, having an anchoring group capable of promoting the chemical adsorption onto TiO_2 surface, improving the electronic coupling between dye and semiconductor interface.

The first DSSC that exhibited $\eta > 10$ % employed *cis*-di(isothiocyanato)bis-(2,2′-bipyridyl-4,4′-dicarboxylic acid)ruthenium(II), N3 as dye-sensitizer [38]. after this dye, the complex *mer*-tri(isothiocyanato)(2,2′,2′'-terpyridyl-4,4′,4′'-tricarboxylic acid)ruthenium(II), black-dye was prepared and also successfully used as sensitizer [39], Fig. 3.

Due to the outstanding performance of N3 and black-dye as dye-sensitizers, they can be used as models for molecular engineering of new dyes. Their chemical attachment onto TiO_2 surface through the carboxylic acid groups of the 2,2′-

bipyridine or of the 2,2′,2′’-terpyridine ligands. Particularly, the 4,4′-dicarboxylic acid-2,2′-bipyridine anchoring ligand is been widely employed among several other possible groups investigated and it has been considered the best one for ruthenium(II) sensitizers [40]. This ligand allows intimate electronic coupling between the dye excited state wavefunction and the semiconductor conducting band. Its lowest unoccupied orbital, LUMO, is the lowest one of the coordination compound and facilitates an efficient electronic transfer of excited dye molecules and Titania nanocrystals [41].

Great influence on the absorption spectra and molar absorptivities of compounds; emission maxima and quantum yields, as well as excited state lifetimes, in addition to the redox properties was observed as a function of the degree of protonation of the carboxylic acids of the ligand. These changes are directly responsible for the increase on photovoltaic performance of solar cells sensitized by N719, Fig. 4, which is the di-deprotonated N3 specie [42]. As a natural consequence, the use of compounds having one or more deprotonated carboxylic groups in the $dcbH_2$ has been increasing [32, 41, 43–48].

Fig. 4 Structure of N719

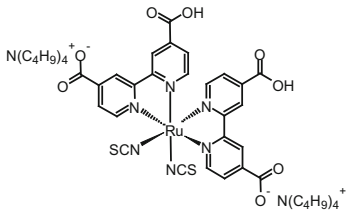

In the case of N3, consequently of N719, the presence of two $dcbH_2$ ligands results in absorption spectra which overlaps the visible region of the incident sunlight. The absorption bands have high molar absorptivity ($\varepsilon \sim 10^4$ L mol^{-1} cm^{-1}), typical of metal-to-ligand charge transfer transitions, $MLCT_{d\pi Ru\text{-}\pi^*dcbH2}$. The high molar absorptivity improves the light harvesting efficiency, allowing the absorption of almost all incidents light in a few micrometers of optical length of the TiO_2 film. Besides the bipyridine, the two isothiocyanate ligands in these complexes are valuable to promote the stabilization of the t_{2g} orbitals and result in a fine tuning of the energy levels of the complex.

3 Ruthenium *Tris*-Heteroleptic Complexes

The knowledge acquired understanding the structure of the N3 dye can be used for the development of several other complexes by using the molecular engineering [49]. Among several classes of compounds developed, ruthenium *tris*-heteroleptic complexes have been gaining attention on the last years due to the possibility to modulate their properties, just changing one of the polypyridinic ligand. This approach is very interesting for the development of new sensitizers.

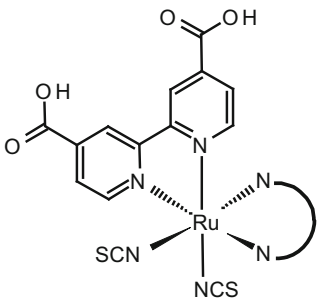

Fig. 5 General structure of cis-[Ru(dcbH$_2$)(L)(NCS)$_2$] dyes

There are several classes of ruthenium *tris*-heteroleptic compounds described by the general formula *cis*-[Ru(dcbH$_2$)(L)(NCS)$_2$], Fig. 5, since each new ligand L and its derivatives can be a new class. In this work, our focus will be on 2,2′-bipyridine derivatives and 1,10-phenanthroline derivatives, even that several other compounds of this general formula is known [34, 50–52].

3.1 2,2′-Bipyridine Derivative Ligands

The search for high-efficiency ruthenium(II) dyes focused on the development of complexes having high molar absorptivity, mainly in visible and near infra-red region [53, 54]. A good light harvesting yield and a reduction on the film thickness, which implies in reduction of transport losses in the nanoporous environment, resulting in higher open-circuit potentials and more efficient devices [55, 56]. Another approach is the development of dye-sensitizers capable of improving the lifetime performance of a dye-sensitized solar cell.

The first *tris*-heteroleptic ruthenium compounds investigated as dye sensitizers are based on 2,2′-bipyridine derivatives and it is possible to observe three different approaches, following the bipyridine substituent. These subclasses are the amphiphilic, donor-antenna and thiophene compounds.

3.1.1 Amphiphilic Compounds

In 2003, a thermally stable DSSC was disclosed employing the amphiphilic Z907 sensitizer. Using this dye was possible to prepare stable devices under prolonged thermal stress at 80°. However, the molar extinction coefficient of this sensitizer is somewhat lower than that of the standard N719 dye. Meanwhile, a compromise between efficiency and high temperature stability has been noted for the Z907 sensitizer [57]. Subsequently, the concept of developing a high molar extinction coefficient, amphiphilic ruthenium sensitizer, was followed by other groups, with a motivation to enhance device efficiency [34, 58–61]. The absorption properties as well as the performance parameters determined for

ruthenium *tris*-heteroleptic complexes having amphiphilic derivatives of 2,2′-bipyridine are listed in Table 1.

The absorption spectra of amphiphilic compounds usually exhibit two MLCT bands in the visible region, typical of ruthenium *bis*-bipyridyl compounds. Molar absorptivity values listed on Table 1 are similar to those determined for the complexes N3 or N719. This behavior is expected since the aliphatic substituents do not have significant influence in the chromophoric properties of the complexes.

Amphiphilic ruthenium *tris*-heteroleptic dye-sensitizers exhibit lower photoelectrochemical performance than determined for N3. The highest efficiency achieved by this class of dyes is 8.6 % [59]. The advantage of these compounds is their long-term stability. These amphiphilic heteroleptic sensitizers have the ground-state pKa of 4,4′-dicarboxy-2,2′-bipyridine higher than determined for N3, enhancing the chemical adsorption of the complex onto the TiO_2 surface [60, 62, 63]. The structure of amphiphilic ligands decreases the charge density on the sensitizer, resulting in less electrostatic repulsion and results in higher amount of dye adsorbed. The hydrophobic substituent of 2,2′-bipyridine does not allow the presence of water molecules close to TiO_2 surface, improving the stabilization of solar cells toward water-induced desorption of the dye. The redox potentials of these complexes are shifted toward a more positive electrochemical potential in comparison to the N3 sensitizer, increasing the reversibility of the ruthenium III/II couple, leading to higher electrochemical stability [60, 62, 63].

3.1.2 Donor-Antenna Compounds

Complexes prepared with donor-antenna substituents of 2,2′-bipyridine are an approach to improve the light absorption at the same time that the hydrophobic character is enhanced. The use of aromatic substituents can have this function since the aromaticity increases the light absorption and the existence of the hydrophobic chain allows the protection to dye desorption caused by water. The spectral and photoelectrochemical parameters of this class of dyes are listed in Table 2.

In most cases it is observed higher molar absorptivities values in comparison to amphiphilic compounds or N3 or N719 dyes which can be ascribed to an extended π-cloud delocalized in the substituent. The higher light harvesting efficiency results directly in higher IPCE values as well as overall efficiency of the solar cell, Tables 2.

There are a few investigations on the use of π-excessive heteroaromatic rings as end-groups in substituted bpy ligands [43, 44, 64]. The use of conjugated π-excessive heteroaromatic rings as end-substituents donors directs the electron injection in the excited state and enhances the oscillator strength resulting in significant increases in the short circuit photocurrent [54].

The higher molar absorptivity in the visible region can be understood by the influence of the different delocalised π-systems integrated in the bipyridyl donor-antenna ligands. The reason for the lower absorption of the standard N719 dye in this region is the absence of any these groups [56].

Table 1 Absorption properties and photoelectrochemical performance of ruthenium (II) *tris*-heteroleptic compounds having amphiphilic derivatives of 2,2′-bipyridine

Abbreviation	Structure	Absorption properties		Photoelectrochemical performance					References
		Solvent	λ_{MAX}/nm ($\varepsilon_{MAX}/10^4$ L mol^{-1}cm^{-1})	V_{OC}/V	J_{SC}/mA cm^{-2}	$IPCE_{MAX}$ (%) (λ/nm)	ff	η_{cell} (%)	
Z907	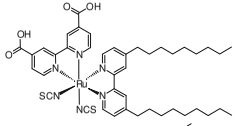	Ethanol	295 (4.24); 312 (3.01); 385 (1.09); 526 (1.16)	0.73	12.5	80 (540)	0.67	6.2	[57]
CS9	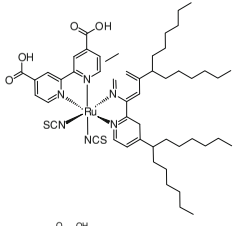	DMF	296 (4.17); 366 (1.03); 518 (0.7)	0.63	14.59	60 (540)	0.62	5.68	[58]
WP-1[a]	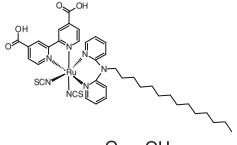	1:1 acetonitrile : tert-butanol	426; 526 (8.7)	0.756	15.5	80 (530)	0.7	8.2	[34]
NMK-2[a]	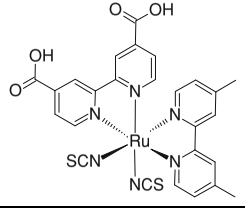	Ethanol	295 (4.54); 312 (3.35); 383 (1.13); 524 (1.16)	0.7	14.7	–	–	6.8	[59]

(continued)

Table 1 (continued)

Abbreviation	Structure	Absorption properties		Photoelectrochemical performance					References
		Solvent	λ_{MAX}/nm ($\varepsilon_{MAX}/10^4$ L mol^{-1}cm^{-1})	V_{OC}/V	J_{SC}/mA cm^{-2}	IPCE$_{MAX}$ (%) (λ/nm)	ff	η_{cell} (%)	
NMK-3[a]	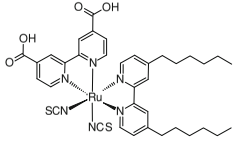	Ethanol	296 (4.26); 312 (3.2); 384 (1.01); 525 (1.11)	0.7	15.5	–	–	7.4	[59]
NMK-5[a]	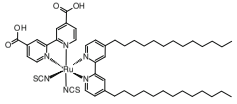	Ethanol	296 (4.21); 312 (3.02); 384 (1.08); 525 (1.15)	0.75	16.2	90	–	8.6	[59]
KC-8[a]	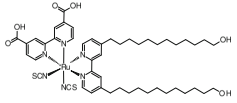	DMF	297 (4.54); 309 (2.74); 370 (1.25); 522 (1.26)	0.673	17.13	86	0.72	8.3	[60]

[a] These compounds were named after the initials of the first author of the reference cited

Table 2 Absorption properties and photoelectrochemical performance of ruthenium (II) *tris*-heteroleptic compounds having donor-antenna derivatives of 2,2′-bipyridine

Abbreviation	Structure	Absorption properties		Photoelectrochemical performance					References
		Solvent	λ_{MAX}/nm ($\varepsilon_{MAX}/10^4$ L mol^{-1}cm^{-1})	V_{OC}/ V	J_{SC}/ mA cm^{-2}	$IPCE_{MAX}$ (%) (λ/ nm)	ff	η_{cell} (%)	
LXJ1	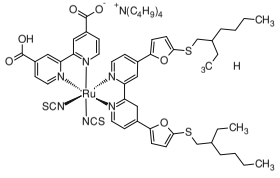	DMF	309 (4.7), 353 (3.3), 549 (1.84)	0.715	16.50	83.7 (550)	0.745	8.80	[43]
IJ-1	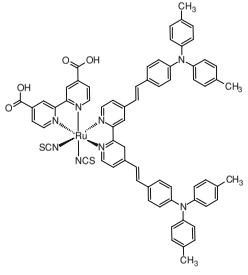	Ethanol	218; 308 (5.0); 432 (4.3), 536 (1.9)	0.748	19.2	87	0.72	10.3	[55]
KW-2[a]	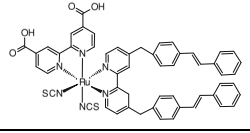	DMF	310 (4.86); 373 (7.95); 550 (2.22)	0.685	3.42	–	0.42	0.99	[56]

(continued)

Table 2 (continued)

Abbreviation	Structure	Absorption properties		Photoelectrochemical performance					References
		Solvent	λ_{MAX}/nm ($\varepsilon_{MAX}/10^4$ L mol^{-1}cm^{-1})	V_{OC}/V	J_{SC}/mA cm^{-2}	$IPCE_{MAX}$ (%) (λ/nm)	ff	η_{cell} (%)	
KW-3[a]	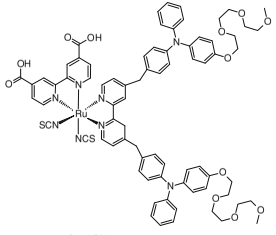	MetOH + 1 wt % KOH	307 (8.13); 429 (5.34); 524 (3.09)	0.735	4.03	–	0.46	1.37	[56]
KW-4[a]	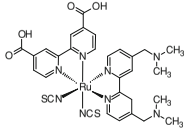	1:1 H_2O:DMF + 1wt % KOH	307 (3.88); 381 (1.28); 526 (1.13)	0.635	2.15	–	0.42	0.58	[56]
KW-5[a]	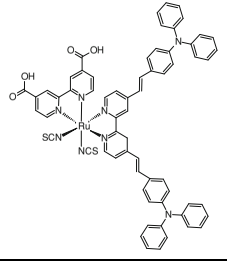	1:1 H_2O:DMF + 1wt % KOH	304 (6.25); 423 (5.47); 544(2.27)	0.715	4.30	–	0.43	1.31	[56]

(continued)

Table 2 (continued)

Abbreviation	Structure	Absorption properties		Photoelectrochemical performance					References
		Solvent	λ_{MAX}/nm ($\varepsilon_{MAX}/10^4$ L mol^{-1}cm^{-1})	V_{OC}/V	J_{SC}/mA cm^{-2}	$IPCE_{MAX}$ (%) (λ/nm)	ff	η_{cell} (%)	
C105	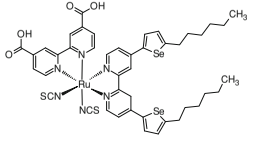	DMF	309 (3.90); 353 (3.2); 420(1.84); 550 (1.84)	0.747	18.9	95 (520)	0.744	10.06	[64]
HRD-1	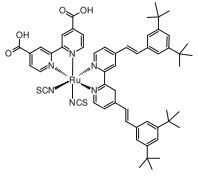	DMF	543 (1.93)	0.59	10.9	60	0.78	4.93	[62]
HRD-2	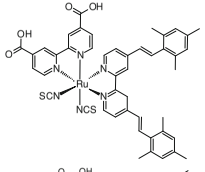	DMF	532 (1.61)	0.60	10.5	64	0.78	4.91	[62]
HRS-2	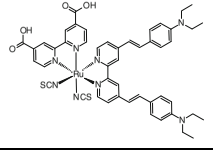	Ethanol	431 (5.93); 542 (2.81)	0.697	17.47	85 (552)	0.711	8.65	[63]

(continued)

Table 2 (continued)

Abbreviation	Structure	Absorption properties		Photoelectrochemical performance					References
		Solvent	λ_{MAX}/nm ($\varepsilon_{MAX}/10^4$ L mol^{-1}cm^{-1})	V_{OC}/V	J_{SC}/mA cm^{-2}	$IPCE_{MAX}$ (%) (λ/nm)	ff	η_{cell} (%)	
C102	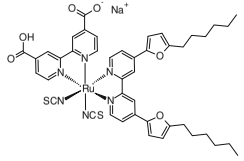	DMF	305; 341; 407; 547(1.68)	0.740	17.80	82 (550)	–	9.5	[44]
AB-1[a]	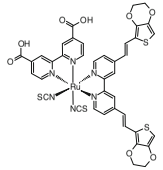	Ethanol	314; 388; 538 (1.6)	0.663	19.1	87	0.72	9.1	[54]
N945	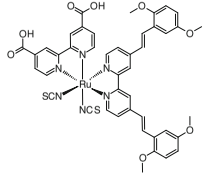	1:1 acetonitrile : tert-butanol	400 (3.4); 550 (1.9)	0.728	17.96	61	0.71	9.29	[76]

(continued)

Table 2 (continued)

Abbreviation	Structure	Absorption properties		Photoelectrochemical performance					References
		Solvent	λ_{MAX}/nm ($\varepsilon_{MAX}/10^4$ L mol^{-1}cm^{-1})	V_{OC}/V	J_{SC}/mA cm^{-2}	$IPCE_{MAX}$ (%) (λ/nm)	ff	η_{cell} (%)	
KCS-1[a]	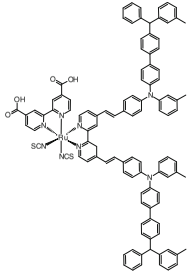	DMF	310 (8.49); 440 (5.34); 540 (2.67)	0.757	9.6	–	0.35	3.4	[77]
K-19	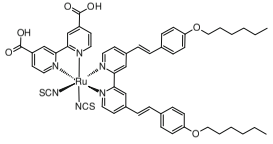	DMF	310 (5.0); 350 (4.8); 410 (1.8); 545 (1.8)	0.718	13.2	–	0.745	7.1	[32]
K-73	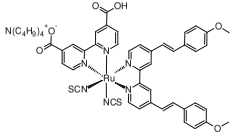	DMF	310; 350; 410; 545	0.748	17.22	85 (540)	0.649	9.5	[32]
Z-910	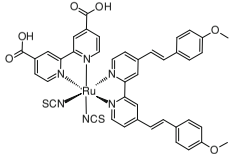	Acetonitrile	410 (1.7); 543 (1.69)	0.777	17.2	87 (520)	0.764	10.2	[33]

(continued)

Table 2 (continued)

Abbreviation	Structure	Absorption properties		Photoelectrochemical performance					References
		Solvent	λ_{MAX}/nm ($\varepsilon_{MAX}/10^4$ L mol^{-1}cm^{-1})	V_{OC}/V	J_{SC}/mA cm^{-2}	$IPCE_{MAX}$ (%) (λ/nm)	ff	η_{cell} (%)	
KC-5[a]	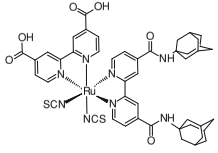	DMF	313 (3.88); 392 (1.17); 537 (1.19)	0.695	15.8	75	0.66	7.01	[60]
KC-6[a]	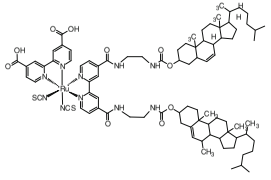	DMF	314 (3.36); 390 (1.11); 531 (1.12)	0.676	15.47	63	0.71	7.42	[60]
KC-7[a]	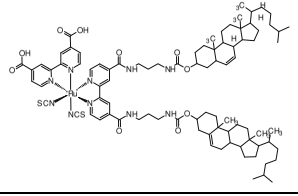	DMF	312 (3.39); 393 (1.12); 533 (1.21)	0.676	16.11	79	0.7	7.62	[60]

[a] These compounds were named after the initials of the first author of the reference cited

3.1.3 Thiophene Compounds

Ruthenium(II) sensitizers having 2,2′-bipyridine with thiophene substituents have higher molar absorptivity than observed for the previous classes of compounds. For instance, the compound KW-1 has $\varepsilon_{515} = 3.56$ L mol^{-1} cm^{-1} [56], much higher than the ones determined for N3 or N719 dyes. As it is observed for the donor-antenna class of compounds, the higher light harvesting efficiency results in higher IPCE values and consequently improve overall performance of the solar cell, Table 3.

Ruthenium(II) thiophene compounds gained special attention after C101 dye has set a new DSSC efficiency record of 11.3–11.5 % and became the first sensitizer to triumph over the well-known N3 dye [44]. In comparison to its analogues C102 or C105, in which the thiophene is replaced by furan, or selenophene, respectively, the molar absorptivity increases in the order of Se > S > O. This sequence it is consistent with the electropositivity trend and the size of the heteroatoms of five-member conjugated units. The LUMO energy sequence of the spectator ligand is O > S > Se, which explain this behavior [64].

Another important dye employing thiophene derivatives is CYC-B1, which exhibts a remarkably high light-harvesting capacity of up to 2.12x10^4 L mol^{-1} cm^{-1} [40]. After the development of the CYC-B1 dye, several ruthenium dyes were synthesized by incorporating thiophene derivatives into the ancillary ligand and DSSC cells based on these dyes exhibited excellent photovoltaic performances [45, 46, 65, 66].

The extensive use of polythiophene is due to its similarity to a *cis*-polyacetylene chain bridged with sulfur atoms. The "bridging sulfur atoms" could effectively provide aromatic stability to the polyacetylene chain while preserving the desirable physical properties, such as high charge transport. The facile functionalization of thiophene groups also offers relatively efficient synthetic solutions to solubility, polarity, and energetic tuning. Furthermore, sulfur has greater radial extension in its bonding than the second-row elements, such as carbon. Therefore, thiophene is a more electron-rich moiety and incorporation of thiophene onto bipyridine ligands raises the energy levels of the metal center and the LUMO of the ligands [67]. As a consequence, the band resulting from charge transfer from the metal center to the anchoring ligand is redshifted, and upon illumination of the sample, the electrons on the metal center are transferred to the anchoring dcbH_2 ligand, where electrons can move to the outer circuit through the TiO_2 particles more efficiently [40].

3.2 1,10-Phenanthroline Derivative Ligands

Besides 2,2′-bipyridine derivatives, 1,10-phenanthroline and its derivatives is gaining attention to be used in *cis*-[Ru(dcbH_2)(L)(NCS)$_2$] sensitizers. Their similarity to 2,2′-bipyridine and the advantage of having an extended π-conjugated structure led to a great potential to be employed as ancillary ligands [68]. This

Table 3 Absorption properties and photoelectrochemical performance of ruthenium (II) *tris*-heteroleptic compounds having thiophene derivatives of 2,2′-bipyridine

Abbreviation	Structure	Absorption properties		Photoelectrochemical performance					References
		Solvent	λ_{MAX}/nm ($\varepsilon_{MAX}/10^4$ L mol^{-1}cm^{-1})	V_{OC}/ V	J_{SC}/ mA cm^{-2}	$IPCE_{MAX}$ (%) (λ/nm)	ff	η_{cell} (%)	
CYC-B1	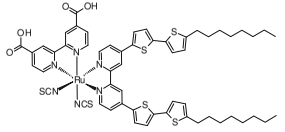	DMF	312 (3.58); 400 (4.64); 553 (2.12)	0.65	23.92	77.5	0.55	8.54	[40]
CYC-B3	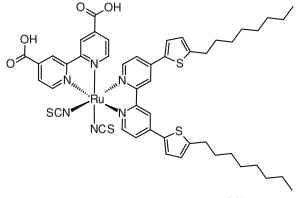	DMF	350; 400; 544 (1.57)	0.669	15.7	64.1 (520)	0.705	7.39	[65]
CYC-B7	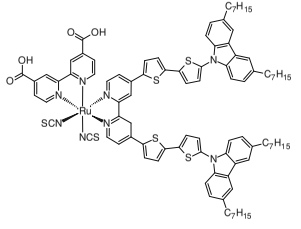	DMF	345 (3.55), 412 (4.35), 551 (2.19)	0.788	17.4	76 (530)	0.654	8.96	[66]
CYC-B11	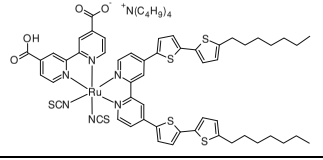	DMF	305(4.5), 388(5.40), 554 (2.42)	0.714	16.1	95 (580)	0.69	7.9	[45]

(continued)

Table 3 (continued)

Abbreviation	Structure	Absorption properties		Photoelectrochemical performance					References
		Solvent	λ_{MAX}/nm ($\varepsilon_{MAX}/10^4$ L mol^{-1}cm^{-1})	V_{OC}/ V	J_{SC}/ mA cm^{-2}	$IPCE_{MAX}$ (%) (λ/nm)	ff	η_{cell} (%)	
CYC-B13	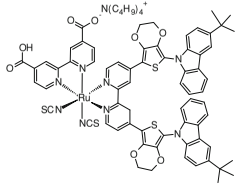	DMF	295 (8.6); 397 (3.4); 547 (1.93)	0.728	10.26	90 (550)	0.68	5.1	[46]
C101	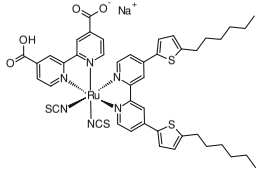	DMF	305; 341; 407; 547 (1.75)	0.746	5.42	89 (580)	0.833	11.3	[44]
C104	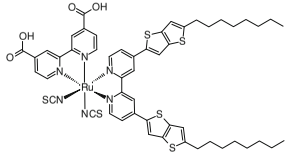	DMF	312 (5.4); 368 (4.5); 553 (2.05)	0.76	17.87	85 (580)	0.776	10.53	[61]
C106	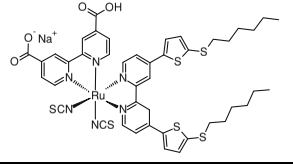	DMF	310 (3.95); 348 (3.1); 550 (1.87)	0.749	18.28	90 (520-640)	0.772	10.57	[41]

(continued)

Table 3 (continued)

Abbreviation	Structure	Absorption properties		Photoelectrochemical performance					References
		Solvent	λ_{MAX}/nm (ε_{MAX}/10^4 L mol^{-1}cm^{-1})	V_{OC}/ V	J_{SC}/ mA cm^{-2}	$IPCE_{MAX}$ (%) (λ/nm)	ff	η_{cell} (%)	
KW-1[a]	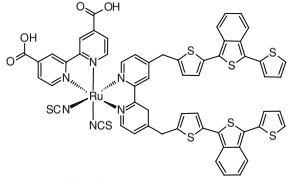	DMF	301 (4.58); 369 (3.51); 515 (3.56)	0,625	1.06	–	0,46	0,31	[56]
RT-1[a]	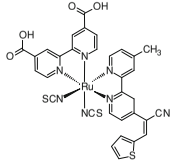	DMF	301 (3.04); 368 (2.28); 529 (1.41)	0.58	6.0	–	0.70	2.45	[78]
RT-2[a]	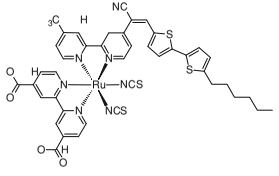	DMF	300 (4.34); 445 (2.88); 551 (1.68)	0.57	5.3	–	0.75	2.84	[78]
RT-3[a]	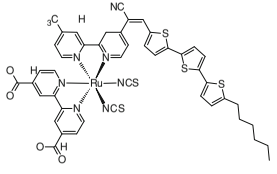	DMF	305 (4.56); 388 (3.15); 563 (2.76)	0.54	4.5	–	0.76	1.85	[78]

(continued)

Table 3 (continued)

Abbreviation	Structure	Absorption properties		Photoelectrochemical performance					References
		Solvent	λ_{MAX}/nm ($\varepsilon_{MAX}/10^4$ L mol^{-1}cm^{-1})	V_{OC}/ V	J_{SC}/ mA cm^{-2}	$IPCE_{MAX}$ (%) (λ/nm)	ff	η_{cell} (%)	
C107	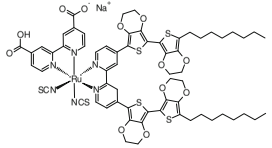	DMF	310 (3.9); 453 (5.43); 552 (2.8)	0.739	19.8	92 (550)	0.751	10.7	[47]
SJW-E1	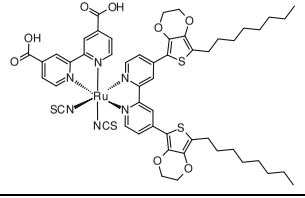	DMF	310; 360; 546 (1.87)	0.669	21.6	72.6 (550)	0.626	9.02	[65]

[a] These compounds were named after the initials of the first author of the reference cited

Table 4 Absorption properties and photoelectrochemical performance of ruthenium (II) *tris*-heteroleptic ruthenium compounds having 1,10-phenanthroline derivatives

Abbreviation	Structure	Absorption properties		Photoelectrochemical performance					References
		Solvent	λ_{MAX}/nm ($\varepsilon_{MAX}/10^4$ L mol^{-1}cm^{-1})	V_{OC}/V	J_{SC}/mA cm^{-2}	$IPCE_{MAX}$ (%) (λ/nm)	ff	η_{cell} (%)	
YS5	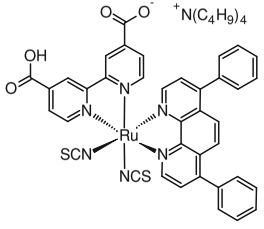	DMF	283(5.68), 308 (3.95), 362 (0,81), 522 (1.71)	0.749	14.52	64.6 (540)	0.557	6.05	[48]
AR25	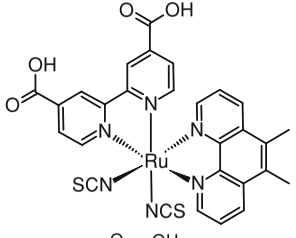	DMF	420; 518(6.58)	0.69	9.6	61 (520)	0.39	2.6	[69]
NOK-1[a]	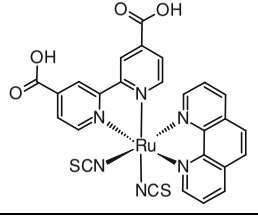	0.01 M NaOH aqueous solution	267 (5.7); 309 (2.9); 400 (1.0); 492(1.2)	0.65	15.3	74	0.67	6.7	[70]

(continued)

Table 4 (continued)

Abbreviation	Structure	Absorption properties		Photoelectrochemical performance					References
		Solvent	λ_{MAX}/nm ($\varepsilon_{MAX}/10^4$ L mol^{-1}cm^{-1})	V_{OC}/V	J_{SC}/mA cm^{-2}	$IPCE_{MAX}$ (%) (λ/nm)	ff	η_{cell} (%)	
NOK-2[a]	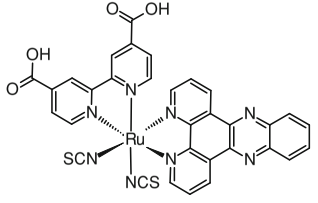	0.01 M NaOH aqueous solution	275 (5.7); 310 (3.5); 374 (1.8); 492 (1.1)	0.62	11.7	54	0.73	5.3	[70]

[a] These compounds were named after the initials of the first author of the reference cited

Table 5 Absorption maxima and photoelectrochemical performance of natural dye-sensitized solar cells reported since 2003

Extract of	Dye	Medium	λ_{max} (nm)	V_{OC} (V)	J_{SC} (mA cm^{-2})	ff	η_{cell} (%)	References
Red-cabbage	Anthocyanin	Water	550	0.52	0.68	0.70	0.50	[79]
Rosella flower	Anthocyanin	Water	520	0.404	1.63	0.57	0.37	[80]
Blue pea flower	Anthocyanin	Water	580, 620	0.372	0.37	0.33	0.05	[80]
Canna indica flower	Anthocyanin	Water and Ethanol	513	0.54	0.82	0.59	0.29	[81]
		TiO_2	530	–	–	–	–	
Salvia splendens flower	Anthocyanin	Water and Ethanol	507	0.558	0.7	0.61	0.26	[81]
		TiO_2	516	–	–	–	–	
Cowberry	Anthocyanin	Water and Ethanol	522	0.556	0.4	0.54	0.13	[81]
		TiO_2	531	–	–	–	–	
Solanum nigrum	Anthocyanin	Water and Ethanol	539	0.54	1.01	0.51	0.31	[81]
		TiO_2	564	–	–	–	–	
Rhododendron arboretum zeylanicum	Anthocyanin	Ethanol	538	0.4020	1.15	0.637	0.29	[82]
Sesbania grandiflora Scarlet	Anthocyanin	Ethanol	544	0.4067	4.40	0.569	1.02	[82]
Hibiscus rosasinensis	Anthocyanin	Ethanol	534	0.4003	4.04	0,633	1.02	[82]
Hibiscus surattensis	Anthocyanin	Ethanol	545	0.3921	5.45	0.535	1.14	[82]
Nerium oleander	Anthocyanin	Ethanol	539	0.4088	2.46	0.591	0.59	[82]
Ixora macrothyrsa	Anthocyanin	Ethanol	537	0.4031	1.31	0.568	0.30	[82]
Black rice	Anthocyanin	Ethanol	560	0.551	1.142	0.52	–	[83]
Rosa xanthina	Anthocyanin	Ethanol	560	0.492	0.637	0.52	–	[83]
Maple leaves	Anthocyanin	Ethanol	536	0.65	1.0	0.60	0.4	[84]
Red Sicilian orange	Anthocyanin	Water	515	0.340	3.84	0.5	–	[85]
Skin of eggplant	Anthocyanin	Water	522	0.350	3.40	0.4	–	[85]
Skin of jaboticaba	Anthocyanin	Ethanol	535	0.66	2.6	0.62	–	[86]
		TiO_2	560	–	–	–	–	
Calafate fruit	Anthocyanin	Water	525	0.47	6.2	0.36	–	[86]
		TiO_2	545	–	–	–	–	
Raw beet	Betalain	TiO_2	470	0.22	2.00	0.51	0.19	[87]
		Water	535	–	–	–	–	

(continued)

Table 5 (continued)

Extract of	Dye	Medium	λ_{max} (nm)	V_{OC} (V)	J_{SC} (mA cm^{-2})	ff	η_{cell} (%)	References
Red Turnip	Betalain	Water	484, 536	0.425	9.5	0.37	1.7	[75]
		TiO_2	450	–	–	–	–	
Wild silician prickly pear	Betalain	TiO_2	460	0.375	8.20	0.38	1.19	[75]
Kelp	Chlorophyll	Ethanol	460	0.441	0.433	0.62	–	[83]
Wormwood	Chlorophyll	Ethanol	432	0.67	2.3	0.56	0.9	[84]
Bamboo leaves	Chlorophyll	Ethanol	432	0.67	1.9	0.56	0.7	[84]
Pomegranate leaves	Chlorophyll	Ethanol	412, 665	0.560	2.05	0.52	0.597	[88]
Curcumin	Polyphenol	Ethanol	430	0.53	0.53	0.72	0.41	[79]
Red-perilla	–	–	–	0.51	0.39	0.67	0.27	[79]
Erythrina	Carotenoid	Ethanol	451	0.484	0.776	0.55	–	[83]
Capsicum	Carotenoid	Ethanol	455	0.412	0.225	0.63	–	[83]
Achiode seed	Carotenoid	Chloroform	440, 475, 500	0.56	0.53	0.66	0.19	[89]

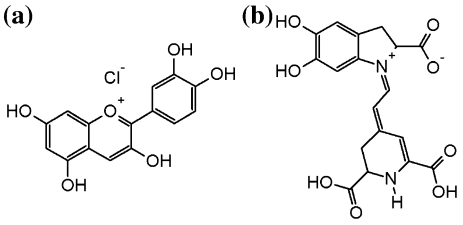

Fig. 6 Structure of anthocyanidin, a flavinic ion of anthocyanin (**a**) and betanidin (**b**), a betalain compound

class of compounds still having few complexes reported in DSSCs, and their spectral as well as photoelectrochemical parameters are listed in Table 4.

The use of phenanthroline derivatives in ruthenium(II) sensitizers leads to properties favorable to the energy conversion processes and can increase on the of DSSCs, which have shown promising results [48, 69, 70].

The comparison on the properties of the complex NOK-1 [70] with N3 indicates that the substitution of the 2,2′-bipyridine derivative by 1,10-phenanthroline does not exhibit better performance or absorption properties. On the other hand, the recently reported complex YS5 exhibits a higher absorbance and also had better performance than the complex N719 under the same condition [48], indicating that this is a promising class of compounds to be investigated.

4 Natural Dyes

Faster, cheaper, low-energy way alternative for ruthenium sensitizers are natural dyes and these compounds has been gaining much attention. Natural dyes can be obtained from fruits, flowers or leaves and are suitable for educational purposes [71, 72] or are an environmentally friendly alternative for dye production since a long-term stability of DSSC using these sensitizers have been demonstrated recently [73].

The absorption properties and photoelectrochemical performance of natural dye-sensitized solar cells reported since 2003 are listed in Table 5.

The most investigated class of natural dyes is the anthocyanins, commonly found in red-purplish fruits or flowers, Fig. 6. These, even other sensitizers have also been investigated [74].

Betalain from raw beet, Red Turnip and Wild silician prickly pear have also been used as natural sensitizers and they have been presented a good photoelectrochemical response, however these cells have low V_{OC}, with overall efficiency up to 1.7 % and reasonable stability [75].

Other classes of natural dyes, such as chlorophyll, polyphenol etc. were also investigated, but the photoelectrochemical parameters were not as good as those observed for anthocyanins or betalains.

5 Conclusion

The energy needs will be supplied by alternative sources and dye-sensitized solar cells are one of the most promising ones for this application since it is cheap and environmentally friendly device. The investigation on dye-sensitizers is fundamental issue on the development of these devices and one of the most promising alternatives is the use of ruthenium *tris*-heteroleptic dyes sensitizers to modulate or enhance their photoelectrochemical performance. The investigation on natural extracts to be employed as dye sensitizers has also been attracting much attention in the last years. They can be an alternative to further reduction of the production costs of these revolutionary devices.

Acknowledgments The authors would like to acknowledge to CNPq (577256/2008-4), FAPESP (2011/11717-8) and UFABC for financial support.

References

1. Cook TR et al (2010) Solar energy supply and storage for the legacy and nonlegacy worlds. Chem Rev 110(11):6474–6502
2. Nocera DG (2009) Chemistry of personalized solar energy. Inorg Chem 48(21):10001–10017
3. Carrette L, Friedrich KA, Stimming U (2000) Fuel cells: principles, types, fuels, and applications. Chem Phys Chem 1(4):162–193
4. Cameron D, Holliday R, Thompson D (2003) Gold's future role in fuel cell systems. J Power Sour 118(1–2):298–303
5. Lemos SG et al (2007) Electrocatalysis of methanol, ethanol and formic acid using a Ru/Pt metallic bilayer. J Power Sour 163(2):695–701
6. Freitas RG et al (2007) Methanol oxidation reaction on $Ti/RuO_{2(x)}Pt_{(1-x)}$ electrodes prepared by the polymeric precursor method. J Power Sour 171(2):373–380
7. Polo AS et al (2011) Pt-Ru-TiO2 photoelectrocatalysts for methanol oxidation. J Power Sour 196(2):872–876
8. Gu C, Shannon C (2007) Investigation of the photocatalytic activity of TiO2-polyoxometalate systems for the oxidation of methanol. J Mol Catal A Chem 262(1–2):185–189
9. Drew K et al. (2005) boosting fuel cell performance with a semiconductor photocatalyst: TiO_2/Pt-Ru hybrid catalyst for methanol oxidation. J Phys Chem B 109(24):11851–11857
10. Kamat PV (2007) Meeting the clean energy demand: nanostructure architectures for solar energy conversion. J Phys Chem C 111(7):2834–2860
11. Armaroli N, Balzani V (2007) The future of energy supply: challenges and opportunities. Angew Chem Int Ed Engl 46(1–2):52–66
12. Meyer TJ (1989) Chemical approaches to artificial photosynthesis. Acc Chem Res 22(5):163–170
13. Dubois DL (2009) Development of molecular electrocatalysts for CO2 reduction and H2 production/oxidation. Acc Chem Res 42(12):1974–1982
14. Morris AJ, Meyer GJ, Fujita E (2009) Molecular approaches to the photocatalytic reduction of carbon dioxide for solar fuels. Acc Chem Res 42(12):1983–1994
15. Concepcion JJ et al (2009) Making oxygen with ruthenium complexes. Acc Chem Res 42(12):1954–1965
16. Walter MG et al (2010) Solar water splitting cells. Chem Rev 110(11):6446–6473

17. Caramori S et al (2010) Photoelectrochemical behavior of sensitized TiO_2 photoanodes in an aqueous environment: application to hydrogen production. Inorg Chem 49(7):3320–3328
18. Koike K et al (2009) Architecture of supramolecular metal complexes for photocatalytic CO2 reduction: III: effects of length of alkyl chain connecting photosensitizer to catalyst. J Photochem Photobiol A Chem 207(1):109–114
19. Takeda H et al (2008) Development of an efficient photocatalytic system for CO_2 reduction using rhenium (i) complexes based on mechanistic studies. J Am Chem Soc 130(6):2023–2031
20. Kroon JM et al (2007) Nanocrystalline dye-sensitized solar cells having maximum performance. Prog Photovolt Res Appl 15(1):1–18
21. Tributsch H (1972) Reaction of excited chlorophyll molecules at electrodes and in photosynthesis*. Photochem Photobiol 16(4):261–269
22. O'Regan B, Gratzel M (1991) A low-cost, high-efficiency solar cell based on dye-sensitized colloidal TiO2 films. Nature 353(6346):737–740
23. Grätzel M (2001) Photoelectrochemical cells. Nature 414(6861):338–344
24. Katoh R et al (2004) Kinetics and mechanism of electron injection and charge recombination in dye-sensitized nanocrystalline semiconductors. Coord Chem Rev 248(13–14):1195–1213
25. Gregg BA (2004) Interfacial processes in the dye-sensitized solar cell. Coord Chem Rev 248(13–14):1215–1224
26. Galoppini E (2004) Linkers for anchoring sensitizers to semiconductor nanoparticles. Coord Chem Rev 248(13–14):1283–1297
27. Anderson NA, Lian T (2004) Ultrafast electron injection from metal polypyridyl complexes to metal-oxide nanocrystalline thin films. Coord Chem Rev 248(13–14):1231–1246
28. Asbury JB et al (2003) Parameters affecting electron injection dynamics from ruthenium dyes to titanium dioxide nanocrystalline thin film. J Phys Chem B 107(30):7376–7386
29. Anderson NA, Ai X, Lian T (2003) Electron injection dynamics from Ru polypyridyl complexes to ZnO nanocrystalline thin films. J Phys Chem B 107(51):14414–14421
30. Garcia CG et al (2002) Electron injection versus charge recombination in photoelectrochemical solar cells using cis-$[(dcbH_2)_2Ru(CNpy)(H_2O)]Cl_2$ as a nanocrystalline TiO_2 sensitizer. J Photochem Photobiol A Chem 151(1–3):165–170
31. Garcia CG et al (2002) Time-resolved experiments in dye-sensitized solar cells using $[(dcbH_2)_2Ru(ppy)_2](ClO_4)_2$ as a nanocrystalline TiO_2 sensitizer. J Photochem Photobiol A Chem 147(2):143–148
32. Kuang DB et al (2006) High molar extinction coefficient heteroleptic ruthenium complexes for thin film dye-sensitized solar cells. J Am Chem Soc 128(12):4146–4154
33. Wang P et al (2004) Stable new sensitizer with improved light harvesting for nanocrystalline dye-sensitized solar cells. Adv Mat 16(20)1806–1811
34. Wang P et al (2004) Amphiphilic polypyridyl ruthenium complexes with substituted 2,2 '-dipyridylamine ligands for nanocrystalline dye-sensitized solar cells. Chem Mater 16(17):3246–3251
35. Pelet S, Moser J-E, Gratzel M (2000) Cooperative effect of adsorbed cations and iodide on the interception of back electron transfer in the dye sensitization of nanocrystalline TiO2. J Phys Chem B 104(8):1791–1795
36. Patrocinio AOT, Paterno LG, Iha NYM (2010) Role of polyelectrolyte for layer-by-layer compact TiO2 films in efficiency enhanced dye-sensitized solar cells. J Phys Chem C 114(41):17954–17959
37. Murakami Iha NY, Garcia CG, Bignozzi CA (2003) Dye-sensitized photoelectrochemical solar cells. In: Nalwa HS (Ed.) Handbook of photochemistry and photobiology. American Scientific Publishers, Stevenson Ranch, p 49–82
38. Nazeeruddin MK et al (1993) Conversion of ligth to electricity by cis-X_2bis(2,2′-Bipyridyl-4,4′-Dicarboxylate)Ruthenium(II) charge-transfer sensitizers ($X = Cl^-$, Br^-, I^-, CN^-, and SCN^-) on nanocrystalline TiO_2 electrodes. J Am Chem Soc 115(14):6382–6390
39. Nazeeruddin MK, Gratzel M (2001) Separation of linkage isomers of trithiocyanato (4,4′,4″-tricarboxy-2,2′,6,2″-terpyridine)ruthenium(II) by pH-titration method and their application in nanocrystalline TiO2-based solar cells. J Photochem Photobiol A Chem 145(1–2):79–86

40. Chen CY et al (2006) A ruthenium complex with superhigh light-harvesting capacity for dye-sensitized solar cells. Angew Chem Int Ed 45(35):5822–5825
41. Cao YM et al (2009) Dye-sensitized solar cells with a high absorptivity ruthenium sensitizer featuring a 2-(Hexylthio)thiophene conjugated bipyridine. J Phys Chem C 113(15):6290–6297
42. Nazeeruddin MK et al (2003) Investigation of sensitizer adsorption and the influence of protons on current and voltage of a dye-sensitized nanocrystalline TiO2 solar cell. J Phys Chem B 107(34):8981–8987
43. Lv XJ, Wang FF, Li YH (2010) Studies of an extremely high molar extinction coefficient ruthenium sensitizer in dye-sensitized solar cells. Acs Appl Mat Interfaces 2(7):1980–1986
44. Gao F et al (2008) Enhance the optical absorptivity of nanocrystalline TiO2 film with high molar extinction coefficient ruthenium sensitizers for high performance dye-sensitized solar cells. J Am Chem Soc 130(32):10720–10728
45. Chen CY et al (2009) Highly efficient light-harvesting ruthenium sensitizer for thin-film dye-sensitized solar cells. ACS Nano 3(10):3103–3109
46. Chen CY et al (2009) New ruthenium sensitizer with carbazole antennas for efficient and stable thin-film dye-sensitized solar cells. J Phys Chem C 113(48):20752–20757
47. Yu QJ et al (2009) An extremely high molar extinction coefficient ruthenium sensitizer in dye-sensitized solar cells: the effects of pi-conjugation extension. J Phys Chem C 113(32):14559–14566
48. Sun YL et al (2010) Viable alternative to N719 for dye-sensitized solar cells. ACS Appl Mater Interfaces 2(7):2039–2045
49. Polo AS, Itokazu MK, Murakami Iha NY (2004) Metal complex sensitizers in dye-sensitized solar cells. Coord Chem Rev 248(13–14):1343–1361
50. Jin Zhengzhe et al (2008) Triarylamine-functionalized ruthenium dyes for efficient dye-sensitized solar cells. ChemSusChem 1(11):901–904
51. Mitsopoulou CA et al (2007) Synthesis, characterization and sensitization properties of two novel mono and bis carboxyl-dipyrido-phenazine ruthenium(II) charge transfer complexes. J Photochem Photobiol A Chem 191:6–12
52. Huang WK et al (2010) Synthesis and electron-transfer properties of benzimidazole-functionalized ruthenium complexes for highly efficient dye-sensitized solar cells. Chem Commun 46(47):8992–8994
53. Wu SJ et al (2010) An efficient light-harvesting ruthenium dye for solar cell application. Dyes Pigm 84(1):95–101
54. Abbotto A et al (2008) Electron-rich heteroaromatic conjugated bipyridine based ruthenium sensitizer for efficient dye-sensitized solar cells. Chem Commun 42:5318–5320
55. Yum JH et al (2009) High efficient donor-acceptor ruthenium complex for dye-sensitized solar cell applications. Energy Environ Sci 2(1):100–102
56. Willinger K et al (2009) Synthesis, spectral, electrochemical and photovoltaic properties of novel heteroleptic polypyridyl ruthenium(II) donor-antenna dyes. J Mater Chem 19(30):5364–5376
57. Wang P et al (2003) A stable quasi-solid-state dye-sensitized solar cell with an amphiphilic ruthenium sensitizer and polymer gel electrolyte (vol 2, pg 402, 2003). Nat Mater 2(7):498–498
58. Sahin C et al (2008) Synthesis of an amphiphilic ruthenium complex with swallow-tail bipyridyl ligand and its application in nc-DSC. Inorg Chim Acta 361(3):671–676
59. Nazeeruddin MK et al (2004) Stepwise assembly of amphiphilic ruthenium sensitizers and their applications in dye-sensitized solar cell. Coord Chem Rev 248(13–14):1317–1328
60. Klein C et al (2004) Amphiphilic ruthenium sensitizers and their applications in dye-sensitized solar cells. Inorg Chem 43(14):4216–4226
61. Gao FF et al (2008) A new heteroleptic ruthenium sensitizer enhances the absorptivity of mesoporous Titania film for a high efficiency dye-sensitized solar cell. Chem Commun 23:2635–2637

62. Giribabu L et al (2009) High molar extinction coefficient amphiphilic ruthenium sensitizers for efficient and stable mesoscopic dye-sensitized solar cells. Energy Environ Sci 2(7):770–773
63. Jiang KJ et al (2008) Efficient sensitization of nanocrystalline TiO2 films with highmolar extinction coefficient ruthenium complex. Inorg Chim Acta 361(3):783–785
64. Gao FF et al (2009) Conjugation of selenophene with bipyridine for a high molar extinction coefficient sensitizer in dye-sensitized solar cells. Inorg Chem 48(6):2664–2669
65. Chen CY et al. (2007) A new route to enhance the light-harvesting capability of ruthenium complexes for dye-sensitized solar cells. Adv Mat 19(22):3888–3891
66. Li J-Y et al (2010) Heteroleptic ruthenium antenna-dye for high-voltage dye-sensitized solar cells. J Mater Chem 20(34):7158–7164
67. Zhu SS, Kingsborough RP, Swager TM (1999) Conducting redox polymers: investigations of polythiophene-Ru(bpy)(3)(n+) hybrid materials. J Mater Chem 9(9):2123–2131
68. Hara K et al (2001) Dye-sensitized nanocrystalline TiO2 solar cells based on ruthenium(II) phenanthroline complex photosensitizers. Langmuir 17(19):5992–5999
69. Reynal A et al (2008) A phenanthroline heteroleptic ruthenium complex and its application to dye-sensitised solar cells. Eur J Inorg Chem 12:1955–1958
70. Onozawa-Komatsuzaki N et al (2006) Molecular and electronic ground and excited structures of heteroleptic ruthenium polypyridyl dyes for nanocrystalline TiO2 solar cells. New J Chem 30(5):689–697
71. Smestad GP, Grätzel M (1998) Demonstrating electron transfer and nanotechnology: a natural dye-sensitised nanocrystalline energy converter. J Chem Educ 75(6):752–756
72. Smestad GP (1998) Education and solar conversion: demonstrating electron transfer. Sol Energy Mater Sol Cells 55(1–2):157–178
73. Patrocinio AOT, Iha NYM (2010) Toward sustainability: solar cells sensitized by natural extracts. Quim Nova 33(3):574–578
74. Zhang D et al. (2008) Betalin pigments for dye-sensitised solar cells. J Photochem Photobiol A Chem 195(1):72–80
75. Calogero G et al (2010) Efficient dye-sensitized solar cells using red turnip and purple wild sicilian prickly pear fruits. Int J Mol Sci 11(1):254–267
76. Nazeeruddin MK et al (2007) A high molar extinction coefficient charge transfer sensitizer and its application in dye-sensitized solar cell. J Photochem Photobiol A Chem 185(2–3):331–337
77. Karthikeyan CS et al (2007) Highly efficient solid-state dye-sensitized TiO2 solar cells via control of retardation of recombination using novel donor-antenna dyes. Sol Energy Mater Sol Cells 91(5):432–439
78. Ryu TI et al (2009) Synthesis and photovoltaic properties of novel ruthenium(ii) sensitizers for dye-sensitized solar cell applications. Bull Korean Chem Soc 30(10):2329–2337
79. Furukawa S et al (2009) Characteristics of dye-sensitized solar cells using natural dye. Thin Solid Films 518(2):526–529
80. Wongcharee K, Meeyoo V, Chavadej S (2007) Dye-sensitized solar cell using natural dyes extracted from rosella and blue pea flowers. Sol Energy Mater Sol Cells 91(7):566–571
81. Luo PH et al (2009) From salmon pink to blue natural sensitizers for solar cells: Canna indica L., Salvia splendens, cowberry and Solanum nigrum L. Spectrochim Acta A Mol Biomol Spectrosc 74(4):936–942
82. Fernando J, Senadeera GKR (2008) Natural anthocyanins as photosensitizers for dye-sensitized solar devices. Curr Sci 95(5):663–666
83. Hao SC et al (2006) Natural dyes as photosensitizers for dye-sensitized solar cell. Sol Energy 80(2):209–214
84. Jin EM et al. (2010) Photosensitization of nanoporous TiO2 films with natural dye. Physica Scripta T139
85. Calogero G, Di Marco G (2008) Red Sicilian orange and purple eggplant fruits as natural sensitizers for dye-sensitized solar cells. Sol Energy Mater Sol Cells 92(11):1341–1346

86. Polo AS, Murakami Iha NY (2006) Blue sensitizers for solar cells: natural dyes from Calafate and Jaboticaba. Sol Energy Mater Sol Cells 90(13):1936–1944
87. Zhang D et al (2008) Betalain pigments for dye-sensitized solar cells. J Photochem Photobiol A Chem 195(1):72–80
88. Chang H, Lo YJ (2010) Pomegranate leaves and mulberry fruit as natural sensitizers for dye-sensitized solar cells. Sol Energy 84(10):1833–1837
89. Gomez-Ortiz NM et al (2010) Dye-sensitized solar cells with natural dyes extracted from achiote seeds. Sol Energy Mater Sol Cells 94(1):40–44

http://www.springer.com/978-3-642-31735-4

Nanoenergy
Nanotechnology Applied for Energy Production
Souza, F.L.; Leite, E.R. (Eds.)
2013, VIII, 200 p., Hardcover
ISBN: 978-3-642-31735-4